33RD INTERNATIONAL COSMIC RAY CONFERENCE, RIO DE JANEIRO 2013
THE ASTROPARTICLE PHYSICS CONFERENCE

Limits to the Gamma Ray Bursts emission in the 1-100 GeV energy range with ARGO-YBJ

T. DI GIROLAMO[1], P. VALLANIA[2], C. VIGORITO[3] FOR THE ARGO-YBJ COLLABORATION.

[1] *Dipartimento di Fisica dell'Università di Napoli "Federico II" & INFN-Napoli, Complesso Universitario di Monte Sant'Angelo, via Cinthia, 80126 Napoli, Italy*
[2] *Osservatorio Astrofisico di Torino dell'Istituto Nazionale di Astrofisica & INFN-Torino, via P. Giuria 1, 10125 Torino, Italy*
[3] *Dipartimento di Fisica dell'Università di Torino & INFN-Torino, via P. Giuria 1, 10125 Torino, Italy*

vigorito@to.infn.it

Abstract: The search for Gamma Ray Bursts (GRB) emission in coincidence with the satellite detection has been carried out since December 2004 by the ARGO-YBJ experiment in both shower and scaler modes. For the latter, a total of 143 events (up to February 7, 2013, end of the ARGO-YBJ data taking) has been analyzed, being up to now the largest sample of GRBs investigated with a ground-based detector. No significant excess has been found, and the resulting fluence upper limits between 1 and 100 GeV can be set as low as 10^{-5} erg/cm^2, comparable at least in one case with the Fermi/LAT measurements. The analysis of a subset of 24 GRBs with known redshift has been used to constrain the fluence extrapolation to the very high energy (VHE) region.

Keywords: gamma ray bursts, gamma ray observations, extensive air shower, RPC detector

1 Introduction

The energy density spectrum of GRBs shows different features, the most important being a peak around a few hundred keV. Nevertheless, EGRET [1] and more recently Fermi [2] and AGILE [3] satellites, have observed photons in the $MeV - GeV$ energy range. At time of writing this paper, the highest energy ~ 94 GeV has been observed by the LAT instrument on Fermi satellite in GRB130427A. Previously, the maximum observed energy was $33.4^{+2.7}_{-3.5}$ GeV in GRB090902B, which had also a distinct spectral component showing a clear deviation from the generally expected Band function, creating a challenge for GRB models [4]. The current models include emission in both internal [5, 6] and external [7, 8, 9] shock scenarios, with γ-rays produced by leptonic or hadronic processes via inverse Compton or neutral pion decay. The spectral slope in the GeV energy region could be of great help in discriminating between different models, in particular the detection of a cutoff energy which has not yet been seen.
At present experimental data in the $MeV - GeV$ energy range come only from satellite experiments. For ground detectors, both Extensive Air Shower (EAS) array and Cherenkov telescopes, the requirement of a sufficient number of secondary particles (electrons or photons), in order to reconstruct the shower arrival direction and primary energy, leads to an energy threshold of at least 100 GeV. A possible technique to reduce the energy threshold of EAS detectors is to work in scaler mode instead of shower mode. The counting rates of the detector are recorded looking for an increase in coincidence with a burst detected by a different experiment. Even if this technique does not allow the reconstruction of the arrival direction and thus an independent search, it benefits of the wide effective area and field of view and very low dead time with an energy threshold typically around 1 GeV, overlapping the highest energy investigated by satellites experiments. The sensitivity is limited but for GRBs observed at low zenith angles is comparable to the highest flux measured by satellites.
The ARGO-YBJ detector has been operated in scaler mode from December 17, 2004 to February 7, 2013. In this period a total of 143 GRBs (selected from the GCN Circulars archive[1]) in the field of view of the detector was investigated searching for an increase in the detector counting rate. No significant excess has been found and the corresponding upper limits to the fluence are presented and discussed.

2 The detector

ARGO-YBJ is an extensive air shower detector located at an altitude of 4300 m a.s.l. (atmospheric depth 606 g cm^{-2}) at the Yangbajing Cosmic Ray Laboratory (30.11°N, 90.53°E) in Tibet, P.R. China. The detector was made by a single layer of Resistive Plate Chambers (RPCs), operated in streamer mode and grouped into 153 units called "clusters" (5.7×7.6 m^2) [10]. Each cluster is made by 12 RPCs (1.23×2.85 m^2) and each RPC was read out by 10 pads, with dimensions 55.6×61.8 cm^2, representing the space-time pixels of the detector. The clusters are disposed in a central full coverage carpet (130 clusters, 74×78 m^2, ∼93% of active surface) and a sampling guard ring (∼40% of coverage) to increase the effective area and improve the core location reconstruction in shower mode.
In scaler mode the total counts are measured every 0.5 s: for each cluster the signal coming from 120 pads is added up and put in coincidence in a narrow time window (150 ns), giving the counting rates of ≥ 1, ≥ 2, ≥ 3, and ≥ 4 pads, which are read by four independent scaler channels. These counting rates are referred in the following as $C_{\geq 1}$, $C_{\geq 2}$, $C_{\geq 3}$, and $C_{\geq 4}$ respectively, and the corresponding rates are $\sim$ 40 kHz, $\sim$ 2 kHz, $\sim$ 300 Hz, and $\sim$ 120 Hz. With four measurement channels sensitive to different mean energies, in case of positive detection valuable information on the high energy spectrum slope and possible cutoff may be directly obtained. Since for the GRB search in scaler mode the authentication is only given by the satel-

1. http://gcn.gsfc.nasa.gov/gcn3_archive.html

lite detection, the stability of the detector and the probability that it mimics a true signal are crucial and have to be deeply investigated.
The main sources of counting rate variations are the pressure, acting on the shower development in the atmosphere, and the ambient temperature, acting on the detector efficiency. The time scale of both variations is much larger than the typical GRB duration (seconds to minutes), so they can be neglected provided the behaviour of the single cluster counting rates is Poissonian. A secondary local effect is due to the radon contamination in the detector hall. Electrons and γ-rays, from short lived radon daughters (mainly $^{214}_{82}Pb$, $^{214}_{83}Bi$, $^{214}_{84}Po$) produced in the radon decay chain, are expected from β-decay and isotope deexcitation. It has been shown that they can influence the cluster counting rates at a level of a few per cent of the reference value. Even in this case the time variations are larger (hours) than the typical GRB duration and they can be neglected in the data processing [11].
A very rapid variation can be induced by nearby lightning. For this reason two electric field monitors *EFM-100*, located at opposite sides of the experimental hall, and a storm tracker *LD-250* (both devices by Boltek industries [12]) have been installed to check the electric field variations.
Details of this study are widely discussed in [13], together with the determination of the effective area, upper limit calculation and expected sensitivity. A detailed description of the analysis procedures can be found in [14] togheter with the results on the first sample of analized GRBs.
The GRB search can be done in both shower and scaler modes; in this paper only the results obtained with the latter are presented and discussed. Shower mode results on a reduced sample of GRBs have been discussed in [15].

3 Data selection and analysis

The ARGO-YBJ detector has been completed in spring 2007 but due to its modularity the data taking started already in December 2004. It ended in February 2013, when the detector has been definitively switched off. In this period a total of 155 GRBs, triggered by satellite detectors, occurred inside the ARGO-YBJ field of view (zenith angle $\theta \leq 45^0$). The present analysis was performed on 143 of them, the missing GRBs belonging to periods when the detector was inactive or not properly working. The distribution of the t_{90} parameter, i.e. the GRB duration in which 90% of photons are observed, is shown in figure 1-a. For 84 of them -the *subset A*- the photon index of the spectrum in the $keV - MeV$ energy region has been measured by satellite instruments, being $<\alpha>=1.6$ the mean value. For 24 events -the *subset B*- the redshift is also known, being $<z>=2.1$ the mean value of this subset. The α and z distribution for the 2 subsets are shown in 1-b and 1-c respectively. The detailed list of GRBs in the subset B is summarized in table 1.

For each GRB the following standard procedure has been adopted: check of the detector stability, cluster selection by quality cuts and significance calculation of the coincident signal in the ARGO-YBJ detector. In order to extract the maximum information from the the experimental data, two analyses have been implemented:

- the coincidence search for each GRB;
- the cumulative search for stacked GRBs.

Details on quality cuts, background, significance calculation and on the analysis technique itself are carefully discussed in [10, 13].

3.1 Coincidence search

The counting rates of the clusters surviving the quality cuts ($<\varepsilon_{cut}>\sim 87\%$ average efficiency over the whole data set) are added up and the normalized fluctuation function

$$f = (s-b)/\sigma, \quad \sigma = \sqrt{b + b\frac{t_{90}[s]}{600}} \qquad (1)$$

is used to give the coincident on-source counts: s is the total number of counts in the t_{90} time window starting at t_0 (i.e. the trigger time) of the signal, both given by the satellite detector; b the number of counts in a fixed time interval $t_0 \pm 300$ s around the signal normalized to the t_{90} duration.
Due to the correlation between the counting rates of different clusters, given by the air shower lateral distribution, the spectra of the sum of the counts are larger than Poissonian. This must be taken into account to calculate the true significance of a signal. The statistical significance of the on-source counts over the background is obtained by studying the fluctuation f in an interval of ± 12 h around the GRB trigger time and using equation (17) of [17]. The accurate description of the signal processing is discussed in [13]. The distribution of the resulting significance for all the 143 GRBs is shown in figure 2.

No significant excess is measured, the most significant event being the GRB080727C with 3.52 $s.d.$ and a post trials chance probability of 3.1%.

3.2 Stacked analysis

Besides the coincidence analysis, a stacked analysis has been done in order to search for common features of all

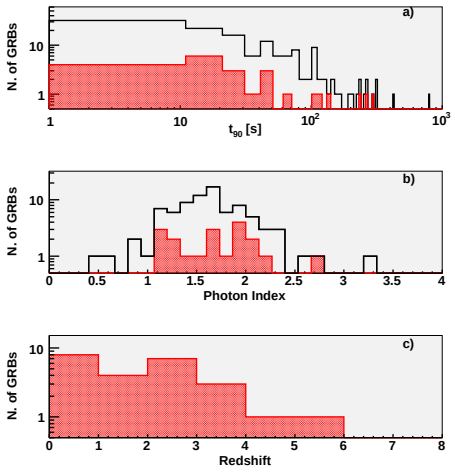

Figure 1: Details of the GRB sample analized in coincidence with ARGO-YBJ: a) t_{90} durations of the whole sample (black line); b) Photon index values for the subset-A (black line); c) redshift value for the subset-B. The dashed red areas correspond to the GRBs with known redshift, the subset-B.

GRB	Sat.	t_{90} [s]	θ [deg]	z	γ-index	n_σ	f_{sat} [$erg\ cm^{-2}$]	$f_{2.5}$ [$erg\ cm^{-2}$]	E_{cut} [GeV]
050408	HETE	15	20.4	1.24	CPL	-2.12	-	$9.1 \cdot 10^{-5}$	-
050802	Swift	19	22.5	1.71	1.54	0.19	$1.0 \cdot 10^{-4}$	$2.1 \cdot 10^{-4}$	8
060115	Swift	139.6	16.6	3.53	CPL	-1.02	-	$7.6 \cdot 10^{-4}$	-
060526	Swift	298	31.7	3.21	2.01	-1.00	$1.8 \cdot 10^{-3}$	$2.7 \cdot 10^{-3}$	-
060714	Swift	115	42.8	2.71	1.93	-0.61	$4.2 \cdot 10^{-3}$	$6.9 \cdot 10^{-3}$	-
060927	Swift	22.5	31.6	5.6	CPL	-0.14	-	$5.1 \cdot 10^{-4}$	-
061110A	Swift	40.7	37.3	0.76	1.67	0.01	$6.7 \cdot 10^{-4}$	$1.7 \cdot 10^{-3}$	-
071112C	Swift	15	18.4	0.823	1.09	1.01	$4.5 \cdot 10^{-5}$	$1.4 \cdot 10^{-4}$	< 2
081028A	Swift	260	29.9	3.038	1.25	0.37	$1.1 \cdot 10^{-3}$	$3.0 \cdot 10^{-3}$	4
090424	Swift	48	33.1	0.544	1.19	0.60	$1.4 \cdot 10^{-4}$	$4.5 \cdot 10^{-4}$	< 2
090426	Swift	1.2	43.7	2.609	1.93	-1.08	$8.0 \cdot 10^{-5}$	$1.3 \cdot 10^{-4}$	-
090529A	Swift	100	19.9	2.625	2.00	-0.66	$2.7 \cdot 10^{-4}$	$4.0 \cdot 10^{-4}$	-
090809A	Swift	5.4	34.2	2.737	1.34	-1.12	$3.5 \cdot 10^{-5}$	$8.8 \cdot 10^{-5}$	4
090902B	Fermi	25	23.1	1.822	1.94	1.09	$1.4 \cdot 10^{-4}$	$2.2 \cdot 10^{-4}$	-
100302A	Swift	17.9	44.6	4.813	1.72	0.04	$1.4 \cdot 10^{4}$	$2.2 \cdot 10^{4}$	
100418A	Swift	7.0	18.7	0.6235	2.16	-1.33	$2.9 \cdot 10^{-5}$	$4.2 \cdot 10^{-5}$	-
110106B	Swift	24.8	25.1	0.618	1.76	2.25	$2.5 \cdot 10^{-4}$	$5.6 \cdot 10^{-4}$	-
110128A	Swift	30.7	43.2	2.339	1.31	2.39	$1.1 \cdot 10^{-3}$	$2.9 \cdot 10^{-3}$	16
111211A	AGILE	15	20.3	0.478	2.77	0.78	$1.8 \cdot 10^{-4}$	$1.4 \cdot 10^{-4}$	-
120326A	Swift	69.6	40.9	1.798	CPL	-0.80	-	$2.2 \cdot 10^{-3}$	-
120716A	IPN	230	35.7	2.486	CPL	-0.57	-	$7.1 \cdot 10^{-3}$	-
120722A	Swift	42.4	17.7	0.9586	1.90	1.23	$1.8 \cdot 10^{-4}$	$3.2 \cdot 10^{-4}$	-
120907A	Swift	16.9	40.2	0.970	1.73	-1.55	$2.4 \cdot 10^{-4}$	$5.6 \cdot 10^{-4}$	-
130131B	Swift	4.30	27.2	2.539	1.15	0.85	$5.2 \cdot 10^{-5}$	$1.4 \cdot 10^{-4}$	< 2

Table 1: GRBs with measured redshift observed by ARGO-YBJ.

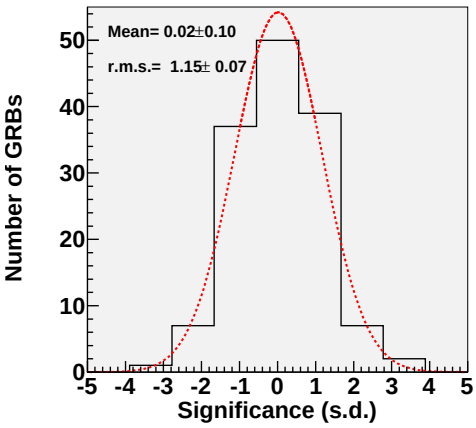

Figure 2: Distribution of the statistical significances of the 143 GRBs with respect to background fluctuations (black full line) compared with a free Gaussian fit (dotted red line). Mean value and r.m.s. of the fit are shown.

GRBs both in *Time* or *Phase*.
In *Time* analysis the counting rates for all the GRBs, in 9 time windows ($\Delta t = 0.5, 1, 2, 5, 10, 20, 50, 100$ and 200 s) starting at t_0, have been added up in order to investigate a possible common duration of the high energy emission. A positive observation at a fixed Δt could be used as an alternative value to the observed t_{90} duration. It can also help to test possible delayed high energy component as indicated by some experimental satellite observations (e.g GRB090510 [16]). The most significant excess (1.9 $s.d.$) is observed at $\Delta t = 0.5s$ with $\sim 26\%$ chance probability .
In the *Phase* analysis only 119 GRBs with duration $t_{90} \geq 5\ s$ have been added up scaling their duration to a common phase plot (i.e. 10 bins each one sampling a 10% wide interval of t_{90} duration, being $0.5s$ the minimum bin duration for the scaler mode data acquisition). This analysis should evidence a common feature of all GRBs in case of a VHE emission correlated with the GRB duration at lower energy. Even in this case no excess is found: the most significant bin, corresponding to the phase $[0.5 : 0.6]$ of the t_{90} duration has a marginal significance of 1.1 $s.d.$.

4 Fluence upper limits

The fluence upper limits can be derived in the $[1 - 100]$ GeV energy range starting from the significance values showed in figure 2 and with some assumptions on the GRB primary spectrum. Since the mean value of the differential spectrum index measured by EGRET in the GeV energy region is $\alpha = -2$, while the average value measured by BATSE at lower energy is $\alpha = -2.36^{+0.22}_{-0.17}$ (see [18]) we used two extrapolations to estimate the expected fluence for each GRB: a) the spectral α_{sat} index measured by satellite detectors in the $keV - Mev$ energy range (f_{sat} fluence values in table 1) and b) the conservative value $\alpha = -2.5$ ($f_{2.5}$ fluence values in table 1). Due to the absorption by the Extragalactic Background Light (EBL) modelled as in [19], an exponential cutoff is applied to the spectrum according to the measured redshift. Figure 3 shows the 99% c.l. upper limits range for the subset-A of GRBs with known redshift. For 5 of them, showing a spectrum better fitted by a Cutoff Power Law (CPL), only the upper limits of case b) are shown.
For GRB090902B (i.e. the GRB in the ARGO-YBJ field of view with the highest energy photon) the integral flux measured by Fermi-LAT in the same energy range is shown. According to our calculation, the extrapolated GRB fluence was just a factor ~ 3 lower than our expected sensitivity.
A comparison between the expected fluence, obtained ex-

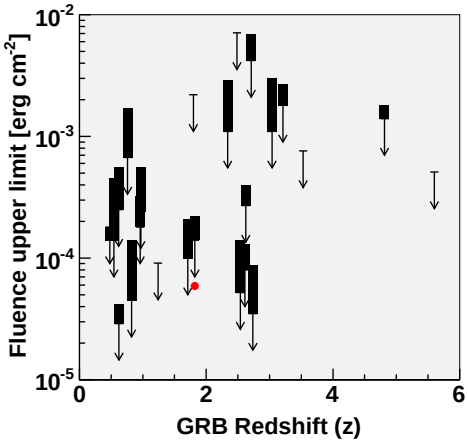

Figure 3: Fluence upper limits of GRBs as a function of redshift. The rectangles represent the values obtained with differential spectral indexes ranging from $\alpha = -2.5$ to the satellite measurement α_{sat}. The 5 arrows give the upper limits for the former case only, these GRBs being better fitted at lower energies with a cutoff power law spectrum. The red dot shows the integral fluence in the 1-100 GeV range for GRB090902B as observed by LAT.

trapolating the $keV - MeV$ measured spectra and including the EBL absorbtion, and the fluence upper limit measured in the ARGO-YBJ scaler data has been done for the 19 GRBs of subset-B with known spectral index. For this analysis the 5 events of subset-B showing a CPL spectrum have been excluded. The result is shown in figure 4.

The line *Upper Limit (UL)= Expected Fluence (EF)* is

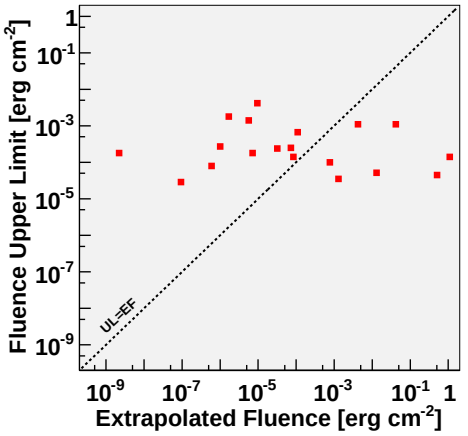

Figure 4: Fluence estrapolation vs the ARGO-YBJ upper limits for the subset-B of GRBs with known redshift.

also drawn. The 7 points on the right side of the line (i.e. in the region where the upper limits are below the extrapolated fluences) indicate that, since the corresponding GRB has not been observed, the assumed extrapolation to VHE is not feasible up to our range $[1 - 100\ GeV]$ or a cut-off energy should be present in the high energy tail of the spectrum. Assuming the spectrum slope according to the low energy measurements the maximum cutoff energy has been estimated. The extrapolated fluence is calculated together with the fluence upper limit as a function of the cutoff energy E_{cut}. If the two curves cross in the $[2 - 100\ GeV]$ energy range, the intersection gives the upper limit to the cutoff energy. For these GRBs and the previous assumptions we can state, with a 99% c.l., that their spectra do not extend beyond this value of E_{cut}. The obtained E_{cut} values are summarized in the last column of table 1. For 3 of them (GRB071112C, GRB090424 and GRB130113B) the estimated E_{cut} upper limit is even below 2 GeV. We can conclude that in these 3 cases the low energy spectrum can not be extended to the GeV region and some additional features occur in the $keV - MeV$ energy range.

Different models for the spectrum and/or different hypothesis on the photon index spectrum in the VHE band can be used. For a more realistic Band spectrum with an E_{break} value of 230 keV and $\alpha = -2,1$, corresponding to the mean peak energy and slope, the 7 GRBs go under threshold (i.e. the extrapolated fluence is always lower than our calcultated upper limit).

5 Conclusions

A search for GRBs in coincidence with satellite detection has been carried out using the complete ARGO-YBJ data set. During 8 years a total of 143 GRBs has been analyzed, the largest GRB sample ever analyzed using this technique. No significant excess has been detected, even if for the GRB090902B the fluence upper limit is close to the LAT measurement. For 7 GRBs of subset-B an upper limit to the cutoff energy has been also set and the average Band spectrum hypothesys has been also tested.

The expected rate of GRBs that can be observed by the ARGO-YBJ experiment, based on the Swift satellite detection, was between 0.1 and 0.5 $year^{-1}$[13] and it should have doubled with the Fermi satellite launch. The value of 0.3 $year^{-1}$ obtained for our 90% c.l. upper limit is close to our lower expectation partially due to the fact that the Fermi detection rate was overestimated and partially to the fact that the Fermi GRBs have a spectrum softer than expected, and a simple extrapolation from low energy is not always possible.

References

[1] Kanbach, G., et al. 1988, Space Sci. Rev., 49, 69.
[2] Meegan, C. et al. 2009, ApJ, 702, 791.
[3] Longo F. et al. 2012, A&A. 547, A95.
[4] Abdo, A. A. et al. 2009, ApJ, 706, L138
[5] Guetta D. et al. 2003, ApJ, 585, 885.
[6] Finke J.D. et al. 2008, AIP Conf. Ser. 1000, eds. M.Galassi, D. Palmer, E. Fenimore, 385.
[7] Kumar P. et al. 2010, MNRAS, 409, 226.
[8] Ghisellini G. et al. 2010, MNRAS, 403, 926.
[9] Guirlanda G. et al. 2010, A&A, 510, L7.
[10] Aielli, G., et al. 2006, NIMA, 562, 92.
[11] X. M. Zhou et al. 2009, Proc. of XXXII ICRC, 11, 287.
[12] http://www.boltek.com/
[13] Aielli, G., et al. 2008, Astr. Phys., 30, 85.
[14] Aielli, G., et al. 2009, ApJ, 699, 1281.
[15] Aielli, G., et al. 2009, Astroparticle Physics, 32, 47.
[16] Giuliani A. et al. 2010, ApJ, 708, L84.
[17] Li, T., & Ma, Y. 1983, ApJ, 272, 317.
[18] Kaneko et al. 2008, ApJ, 677, 1168.
[19] Kneiske et al. 2004, A&A, 413, 807.